A Pulse Oximeter

João Carreiras

Dept. of Bioengineering, IST, Lisbon, Portugal

June 11, 2013

Keywords: Pulse Oximetry, Oxygen Saturation, Digital Signal Processing

1 Introduction

The objective of this work is two fold: the development of a pulse oximeter capable of measuring the S_aO_2, heart rate and displaying the oximetry wave; conversion of this prototype into an oximeter capable of measuring the CO_2 concentration in blood. The S_aO_2, measured by oximetry and defined as the relative amount of O_2 carried by the hemoglobin, is one the most important biomedical signals in patient monitoring. It is a standard in any operating room, ambulance, intensive care unit and indicated for both perioperative and postoperative monitoring [1] [2].

This project unfolded in several stages, comprising the construction of the initial pulse oximeter prototype, its calibration and the attempt to measure CO_2, which was not accomplished.

This summary begins with an introductory chapter, followed by a presentation of the prototype and the results obtained with it. Finally, a discussion of the results and future directions will be presented.

2 Prototype

In this chapter, an explanation of the developed prototype will be given, the electronic components utilised and choices made. The development can be divided into four parts: excitation stage, detection stage, digitalisation and signal processing, all depicted in figure 1.

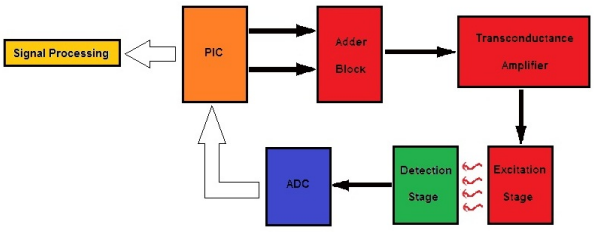

Figure 1: Block Diagram of the Prototype. The black arrows represent analog signal, the white arrows represent digital signal and the red arrows are light photons.

As can be seen in figure 1, firstly one needs to produce a signal for the LEDs, followed then by its detection and digitalisation into microcontroller language, to be ready for processing.

2.1 Excitation Stage

To create the signal which will be transmitted through the vascular bed and interact with the hemoglobin molecule, a specific circuitry is required. Two pins of the microcontroller were set as digital outputs, each one originating a rectangular wave of 3.3 V and 10% duty cycle that will excite the red and infrared LEDs. The timing diagram will have then a positive pulse, a negative and a no-pulse stage, which will act as a measure of the noise from ambient light and dark current.

These signals have a 500 Hz frequency, to be capable of detecting all the small changes in the pulsatile blood waveform, and must be time shifted by 400 μs, in order to allow the photodetector to distinguish between them.

However, the LEDs are arranged in an antiparalell configuration, meaning that they have reversed polarities with respect to one another. In this way, only one LED will emit at a given time, thus allowing for the separation between red and infrared signals with only one input wire on the sensor. With this configuration, when one diode is conducting, the other one is cut due to reverse bias current [4].

Even though the antiparalell configuration provides a solution, it also raises a problem: the two existent signals need to be added and one of them has to be reversed. For solving said problem, an adder block (*vid.* figure 1) was included in the prototype, allowing the addition of the two rectangular waves as well as reversing one of the signals.

Following this stage, there is a voltage-to-current amplifier stage devised to impose a constant input current on the LEDs. In order to do it, a resistor of a specific value will have to be put between the ground, the diodes and the inverting entrance of the amplifier. This will limit the current on the LEDs as intended, thus preventing the diodes from fusing. The maximum current is 300 mA, hence the resistor value chosen was 6.8 Ω.

Following the excitation signal's creation, the LEDs will be illuminated sequentially. The model chose for the red LED was a general purpose 5 mm bright red LED with a peak wavelength of 640 nm and a 1 A maximum peak forward current. The chosen LED for the infrared region has a peak wavelength of 935 nm and a spectral bandwidth at half maximum of 50 nm. It has a good enough rise time and fall time given an excitation pulse has 200 μs duration, thus the signal is barely affected.

2.2 Detection Stage

In this section, one will deepen the explanation behind the photodetector and associated circuitry. After leaving the emitter, light will travel through the tissue crossing skin, muscles, bone and blood, only to be received on the other end by the receptor. The detection stage is thus comprised by the receptor and an amplifier that will convert this signal for further processing.

When choosing the photodiode, one must take into account several factors such as its spectral response, which should be broad enough to cover the wavelengths typically utilised in pulse

oximetry but, at the same time, it should not cover more than necessary. Sensitivity is also an important parameter due to the low SNR existent. It is expressed as the output current for a known irradiance and it depends naturally on temperature but also on the dark current.

The latter parameter is defined as the reverse current present in the total absence of light. It obviously contaminates the readings and directly decreases the sensitivity of the photodiode [4].

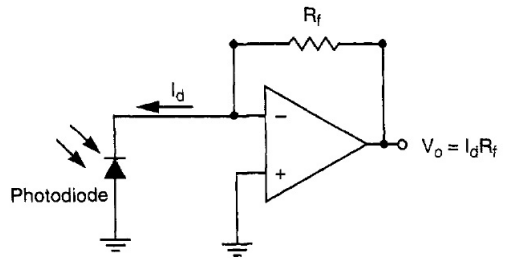

Figure 2: Transimpedance Amplifier Circuit Diagram [4].

However, following the photocurrent production, it becomes necessary to convert that current into a voltage for the microcontroller to work with. This is achieved by implementing a current-to-voltage amplifier circuit, as seen in figure 2.

Taking advantage of the Operational Amplifier virtual ground the photocurrent flows straight through the feedback resistor, R_f, and produces a voltage proportional to the light intensity

On the present project, there is a specific photodiode for each LED: red and infrared signals. This pair was assembled in a silicon substract, to protect both photodiodes, and with only one wire as output.

The combined photocurrent will be amplified by the AD8610 making the signal ready for digitalisation.

Withal, given the high sensitivity, high input impedance of said circuit, the noise coupling can be of two types: capacitive coupling derived from any AC voltage sources, and magnetic coupling from loop areas and long connections, which are avoided as much as possible during prototype development.

An important characteristic to point out is the common-mode rejection ratio of 95 dB, which makes this Op Amp good at picking up the AC signal among some possible common-mode noise.

2.3 Digital Conversion

Following the reception and conversion of the photocurrent into voltage, the next step will be to digitalise said signal.

In the past, all processing of signals was done in analog form, which is prone to noise and interference. Nowadays, due to processors and microcontrollers this processing is all done in a digital manner: calculations and digital filtering algorithms, for example. Furthermore, the digitalisation completely eliminates the influence of noise over several operations because it univoquely determines a set of discrete values (in time or frequency) for the analog signal considered [5].

To perform this task the electronic component utilised is an ADC. Typically available as a single IC ready to use, ADCs convert the voltage levels into bits and send them to the microcontroller.

The physical process behind conversion is

called sampling and the sample numbers are multiples of a basic increment, equivalent to the least significant bit(LSB). Each consecutive bit represents an increase in this basic increment.

In the present work, the ADC chosen was the AD977A from ©Analog Devices. It features low dissipation, an internal reference and several possible input ranges, of which the chosen one will be $\pm 5V$ to cover the registered values.

A good enough discrimination for the signals being measured can be obtained with 16-bit resolution. It is important to note, however, that the ADC's bandwidth is 1.5 MHz, thus the resolution will be slightly inferior, though not compromising the signal's digitalisation. The effective number of bits is also related to the signal-to-noise and distortion ratio which is 83 dB for the AD997A, a good value [6][7].

Furthermore, the AD977A has a maximum throughput rate of 200 kSPS (samplings per second), thus allowing for high sampling frequencies and minimising the aliasing. This effect occurs when, for a limited band signal, the sampling frequency is smaller than twice the signal's maximum frequency - Nyquist theorem [8][7]. In this project the sampling rate will be 20 KHz which means that for each 400 μs excitation step 8 samples will be taken .

2.4 Data Transfer and Signal Processing

Afterwards, the S_pO_2 digitalised waveform is directed to the microcontroller. In this section, an overview of the embedded code will be given, as well as the communication protocol between the microcontroller and the computer, finishing by explaining the algorithms developed to process the signal and extract relevant information from it.

First, the UART sends 8 data bits in each transmission. However, the data's format in memory is 16-bit. Hence, the data is separated into two 8-bit numbers, in order to send them via UART to the computer. Afterwards, data are sent via USB, and to receive them a Matlab®routine was developed, which sets a baudrate equal to the microcontroller's baudrate and creates a receiving buffer. Furthermore, this reconstruction is stored in a vector, which will then pass a series of processing steps to recover the arterial blood pulsatile waveform and the S_pO_2.

The algorithms presented below will try to eliminate the noise and artifacts contaminating the pulse oximetry waveform.

Firstly, data will be truncated in an attempt to eliminate obvious sets of outliers possibly resulting from some interference in the transmission, distortion in amplification circuit or sudden finger movement.

Next, a median filter with a 3 data points window will be applied. The operation manner of this filter is that it accesses a specific point n and, in a window of $\pm w$ data points, returns as its output $y[n]$ the median of said values. The median filter can then be defined as

$$y[n] = median(x[n-w], \cdots, x[n], \cdots, x[n+w]) \quad (1)$$

This approach is excellent to deal with outliers because it can suppress isolated noise (one or two data points at most) without blurring the sharp edges [9] or corrupting signal trends[10]. Even though it is widely utilised, median filtering should only be applied in a signal that is not highly contaminated with noise.

On Matlab®, this filter was developed by going through the whole signal and computing the median with $w = 3$ while taking special attention to the values of the vector that are in the edges. In figure 3, it is possible to visualize its effect. Several spikes resulting either from the digital conversion or the communication were all eliminated and a much clear signal appears afterwards.

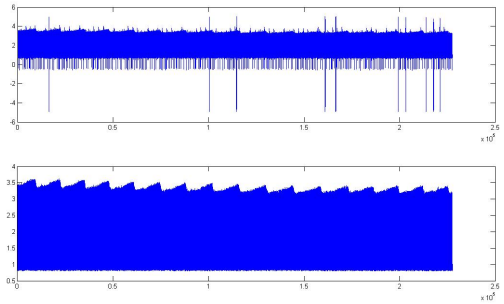

Figure 3: Top: signal before filtering. Bottom: signal after median filter application.

The following step consists in dividing the data into red and infrared. As previously stated (*vid.* section 2.1), there was a need to join the red and infrared excitation signals, so now one needs to split them up.

There is more light absorption at the red wavelength compared to the infrared(IR). Naturally, this characteristic will allow a separation of the two waveforms by a threshold-based approach with empirical values in order to reconstruct the waveform.

Following the threshold separation, the waveform is similar to a rectangular wave with various values for its pulses. The baseline is not zero; instead it corresponds to noise sources, such as dark current. What will be performed next is a decimation process necessary to show the traditional pulsatile waveform. This will happen by computing the average for each pulse and subtracting the noise average in the immediate vicinity of the pulse - just before and after it.

Once the signals are separated, the pulsatile waveform for red and for IR takes shape, though still highly contaminated with noise. Most of the next steps are almost standard in the signal processing of any biomedical signal.

Firstly, there is a need to remove what is usually called the baseline trend. This type of trend in oximetry might be associated with small movements (slight hand tremor). The mathematical approach to this problem is to use a polynomial fit, that is, an interpolation of a data set with a polynomial. Here, one wants to eliminate the baseline trend. Hence a 1^{st} order polynomial is the ideal. A higher order polynomial would only hinder the attempts to pick and eliminate the baseline trend, because it would fit other components of the signal (overfit) and even alter the waveform dramatically, thus eliminating information.

Secondly, one needs to eliminate the high frequencies, making use of the well-known moving average filter, given by expression 2

$$y[n] = \frac{1}{w+1} \sum_{k=-\frac{w}{2}}^{\frac{w}{2}} x[n-k] \qquad (2)$$

This FIR filter corresponds to a simple convolution of a set of coefficients with the input signal for all the points inside of a window w centered in n. In this case, the coefficient simply is $\frac{1}{w+1}$, with w the number of data points of the window, thus computing an average for each datum point. However, this filter will act as a low-pass filter, smoothing the signal [11]. The greater the window w, the smoother the signal will become, so it is important to have that in mind in order to prevent loss of the original signal's characteristics.

The Matlab®implementation is in every way similar to the median filter with the exception of utilising the mean function to compute the average, instead of the median, as seen in figure 4. One can observe the clear smoothing of the signal. This step transforms a still rather noisy and inconstant signal into a closer version of the theoretical photoplethysmografic(PPG) waveform.

Afterwards it was calculated the mean by periods of the signal and that value was subtracted from the data. Following all these steps, the signal looked like a pulsatile waveform typical of pulse oximetry and one could calculate the several parameters of interest.

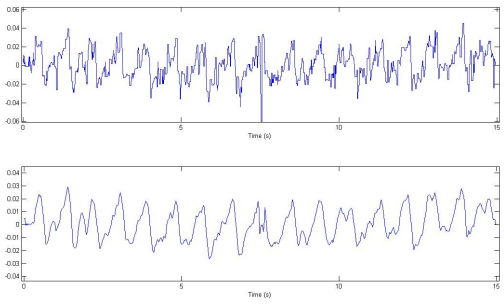

Figure 4: Top: IR signal before filtering. Bottom: IR signal after mean filter application.

A calculation of the maxima ensued, by making use of Matlab's®*findpeaks* function. These peaks are associated with cardiac cycle and so were then counted and divided by the time period, thus giving the heart frequency.

To calculate the S_pO_2 was utilised an empirical expression, after calibration.

3 Results and Discussion

3.1 Calibration

To calibrate the prototype, the values measured with the oximeter were compared with a comercial monitor - the ©Task Force Monitor. Among other biomedical signals, this system is capable of recording and saving S_pO_2 data. Later, these data were utilised to compute a regression equation of the form of

$$S_pO_2 = 97 + \frac{10R}{2+R} \qquad (3)$$

3.2 Results Display

To improve user interface and display the results, a Graphical User Interface (GUI) was built. The GUI allows the user to interact through simple buttons and images with the device. This one

simply consisted of a START button to run the display, two plots of red and infrared PPG wave recordings and the heart rate and S_pO_2 measurements, as can be seen in 5.

The script runs and displays the different recordings in almost real-time. Below there is an example (Figure 5) of data gathered. The visualization window is 5 seconds, the heart rate is calculated for that window and the S_pO_2 is a mean value for this time period.

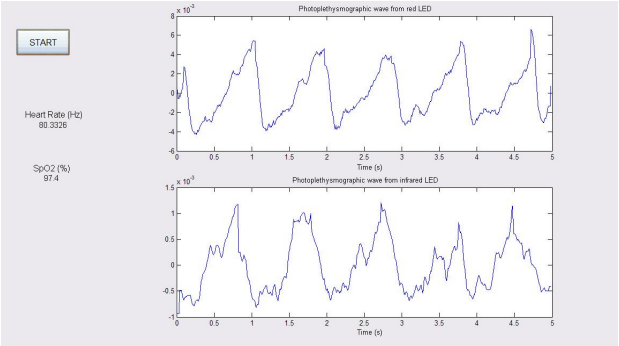

Figure 5: GUI functioning in real-time.

Below there is a 1-minute recording during normal breathing of the PPG waveform

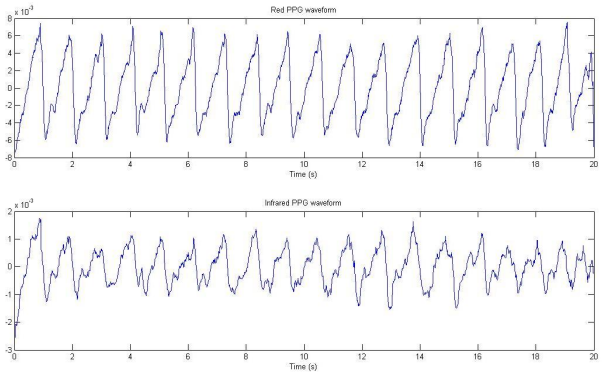

Figure 6: Red(top) and infrared(bottom) PPG waveforms during normal breathing.

and its corresponding calculated S_pO_2

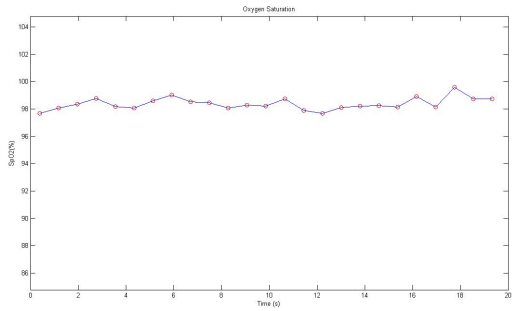

Figure 7: S_pO_2 recording during normal breathing.

3.3 Discussion

In figure 6 both red and infrared waveforms are very clear and show the expected "saw-tooth" like appearance.

When the red signal is at a maximum the infrared is at a minimum, which was expected. One can verify that Hb absorbs more red light while HbO_2 is the opposite. Thus, each red peak corresponds to low concentration of Hb and, consequently, higher S_pO_2 measured. At the same time, infrared must be at a minimum because with higher oxygen saturation the absorbance at infrared wavelength will increase, thus the signal transmitted to the photodetector will be smaller.

In another experiment, the subject held his breath as much as possible. Although the red wave form was well captured, the infrared signal was noisier than the normal breathing.

As can be seen in figure 5 the heart rate was well computed by the algorithm. In both trials, PPG waves one can assess different heart rates by simply inspecting the plots. When holding breath, the subject is put into a stress situation and the increase in heart rate is easily visible with more peaks in the same 20-secs window.

The oxygen saturation was computed from

the calibration made in section 3.1. As can be seen in figure 7, the recorded S_pO_2 is around 98%, which is standard for healthy individuals as our subject.

Concerning the results obtained, one can draw the following critics: since the calibration was done via comparison and not by utilizing known O_2 concentration solutions the results cannot be completely accurate. The technique of holding breath is also highly unpredictable and one cannot hold the breath enough time to produce significant and measurable changes.

Moreover, the electromagnetic isolation was not ideal which may have corrupted the data and influenced the results.

4 Conclusions and Future Work

After many setbacks, the current project has been able to accomplish the main objective of developing a pulse oximeter capable of registering the cardiac frequency, the PPG wave and calculate S_pO_2. The control is performed by a microcontroller and a several step algorithm was implemented. All this is interfaced via an easy-to-use ©Matlab's GUI. The results obtained were satisfactory and the prototype was calibrated by utilising a medical monitor.

However, this thesis was not able to test the possibility of performing a spectrographic-based measure for CO_2 the same way pulse oximetry is performed nowadays. Concerning this particular issue, there have been problems with the LEDs utilised because they were highly sensible and were damaged a couple of times. On top of this, there was some debate around the fact that in blood CO_2 is mainly carried via the blood-tampon system. This would mean that the molecule to be measured should be the hydroxicarbonate, HCO_3^-.

If such a device as was proposed at the beginning of this project was developed, its applicability would be enormous. Assessing the CO_2 is of paramount importance and research in this field should procceed despite the setbacks encountered. It remains to be seen whether the molecule of interest is the CO_2 or of hydroxicarbonate and further research into the best possible wavelength should be conducted. Whichever suits best the purpose of measuring CO_2 saturation in blood should be chosen.

Whichever the molecule to be measured, the excitation and reception circuitry must be well studied because for sure there were interferences maybe concerned with air. One should remember that water has a strong absoprtion band in mid-infrared which can severly damage signal's strength.

Since the developed prototype was built in a modular way, it is possible, for instance, to develop a cuff that encircles the blood vessel and simply connect it to the rest of the prototype. A wireless communication module could have also been developed as it improves the usability and utility of pulse oximeters, as can be seen in comercialized models.

The implemented algorithm can always be upgraded by further implementing code in the microcontroller to correct for temperature drift,

to increase recording speed, etc. On ©Matlab, more advanced techniques can be utilized to extract more information from the PPG wave.

References

[1] Y. Pole, "Evolution of the pulse oximeter," *Int. Cong. Series*, 2002.

[2] T. P. et al, "Pulse Oximetry for Perioperative Monitoring: Systematic Review of Randomized, Controlled Trials," *Anesth Analg*, 2003.

[3] R. B. Jr., "Printed Circuit Boards Part I - Overview," 2004.

[4] J. W. et al, "Design of Pulse Oximeters," *Medical Science Series*, 1997.

[5] A. Sedra and K. Smith, "Microelectronics Circuits," *Oxford University Press.* 5^{th} *edition*, 2004.

[6] "Digital-Analog Conversion - Introduction," *All About Circuits.*

[7] R. Martins, "Apontamentos de Instrumentação e Aquisição de Sinais," 2009-2010.

[8] I. Lourtie, "Sinais e Sistemas. 2Âª Edição," *Escolar Editora.*, 2007.

[9] R. Wang, "Median Filter," http://fourier.eng.hmc.edu/e161/lectures/smooth_sharpen/node4.html, September 2011.

[10] Wesley, *Dr. Dobb's Journal*, October 1999.

[11] J. Semmlow, "Biosignal and Biomedical Image Processing MATLAB based Applications," *Marcel Dekker, Inc.*, 2004.